

Frequency Index Modulation for Low Complexity Low Energy Communication Networks

EBRAHIM SOUJERI^{1,2}, (Senior Member, IEEE), GEORGES KADDOUM¹, (Member, IEEE), MINH AU¹, AND MARIJAN HERCEG³, (Member, IEEE)

¹University of Québec, ÉTS, LaCIME Laboratory, Montreal, H3C 1K3, Canada

²Department of Electrical and Electronics Engineering, European University of Lefke, Northern Cyprus, Turkey

³Department of Communications, Faculty of Electrical Engineering, Computer Science and Information Technology, Osijek, Croatia

Corresponding author: Ebrahim Soujeri (esoujeri@ieee.org)

ABSTRACT In this paper, we propose a low-complexity multi-user communication system based on frequency index modulation that suits Internet of Things applications. This system aims to reduce the transmitted energy and the peak-to-average-power ratio (PAPR) of orthogonal frequency-division multiplexing (OFDM) systems and to perform without sacrificing data rate in comparison with conventional OFDM. In this design, OFDM-like signals are used to make the implementation of the system easy by the virtue of fast Fourier transform (FFT). In the proposed scheme, an OFDM bandwidth of N_{FIM} total sub carriers is divided into N_B equal number of sub-bands, with N subcarriers in every sub-band. At the transmitter side of each sensor, the outgoing bit stream is divided into two blocks: mapped and modulated. The bits within the mapped block are used to activate the corresponding subcarrier in its predefined sub-band in order to carry the data content of the modulated block, while the other $N - 1$ subcarriers are nulled out. At the receiver, the FFT is performed first, and then the square-law envelope detector is applied to estimate the active frequency index to recover the mapped bits, followed by a conventional demodulation process to demodulate the transmitted bits. Once the system is presented and analyzed, energy efficiency, PAPR and complexity are studied to show the features of the proposed scheme. Moreover, we derive closed-form expressions of the bit error rate performance over Rayleigh fading channels and we validate the outcome by simulation results. With the characteristics exhibited in this paper, the proposed system would constitute an excellent candidate for wireless sensor applications where it represents a simpler substitution for frequency-hopping-based architectures, in which the hops carry extra bits.

INDEX TERMS Index modulation, frequency hopping, WSN, IoT, energy efficiency.

I. INTRODUCTION

Recently, there has been an escalating demand for higher data rate communication systems that is associated with an increasing need in the number of devices, gadgets and wireless services. On the one hand, the 5G infrastructure public private partnership has set the goal of reaching 1000 times more speed compared to what we had in 2010, while the power to-be-consumed to run such networks are desired to be around 10% of the consumption at that time [1]. On the other hand, the concept of internet of things (IoT) has advanced in parallel to the developments in 5G networks by virtue of wireless sensor networks (WSN) that have emerged as the most promising technologies for the future that touch various aspects of our life like fitness, automation, security, localization, consumer electronics, smart grid devices and many more [2]. In fact, WSNs have been among one

of the most researched areas in the last decade. The emergence of this technology has only been possible via advances in and availability of small, inexpensive and smart sensors that are cost effective and easily deployable [2]. Various modulation types have so far been used in wireless sensor nodes, among these schemes are M -ary quadrature amplitude modulation (MQAM), offset quadrature phase-shift keying (OQPSK) and multiple frequency-shift keying (MFSK), which is also known as the *green modulation* scheme providing the advantage of low complexity and low cost of implementation in comparison to other schemes [3].

It is to be mentioned that in order to increase data rate, alternative index modulation schemes such as spatial modulation, code index modulation, subcarrier-index modulation, etc, have been proposed to achieve both high data rate and energy efficiency in emerging networks. To achieve this goal,

indexing certain parameters of the communication system into the transmission mechanism in order to enable the conveyance of extra bits per symbol, at neither exaggerated bandwidth cost nor increased transmission power cost has been seriously considered in the last decade.

In this context, spatial modulation (SM) which uses index modulation by multiple antennae in order to increase the data rate and partially enhance the transmission capacity, has been considered in [4]–[7]. In this approach, antenna number or antenna index is used as an extra parameter to convey information and enhance transmission data rate. At each transmission instant, only one transmit antenna in the set is active while all other antennae are inactive. Nonetheless, this scheme has not been cost-free either, since it totally depends on the channel characteristics, requires a continuous *update* of the CSI which imposes noticeable transmission overheads [8] and is very fragile with respect to both noisy CSI estimation as well as correlated channels [9], [10]. Besides, switching time is a major impediment that caps the ambitions related to the implementation of this system in real-life scenarios. The recent study of [11] has shown that switching time, i.e. the duration of time needed by RF switches to carry out transitions between antennae, limits the ambitions of SM and introduces noticeable gaps between projected and actual data rates.

Furthermore, code index modulation-spread spectrum (CIM-SS) has also been proposed as an alternative index-based modulation to achieve higher throughput [12]. This system uses spreading codes to map the data in conjunction with the constellation symbols. In this configuration, bits are grouped into two categories, mapped bits and modulated bits. Mapped bits choose a spreading code from a set of predetermined codes in order to spread the modulated bit. At the receiver, the spreading code is first detected using the maximum autocorrelation value and then the transmitted bit is demodulated.

Additionally, subcarrier index modulation (SIM) scheme has been proposed in [13] where it is merged with orthogonal frequency division multiplexing (OFDM) to constitute SIM-OFDM. Moreover, enhanced subcarrier index modulation (ESIM) has been proposed to avoid the propagation of error by replacing the concept of majority counting by a simpler method in which a pair of *off-on* or *on-off* subcarriers is used to represent a single bit [14], however, the fact that two subcarriers are used to transmit a single bit doubles the required bandwidth necessary for transmission in this method.

Eventually, a transmission scheme called OFDM with index modulation (OFDM-IM) is proposed [15]. In this scheme, information is conveyed not only by M -ary signal constellations as in classical OFDM, but also by the indices of the subcarriers, which are activated according to the incoming information bits. But the implementation of this last scheme is hard as it relies on the maximum likelihood (ML) detection that requires a lot of computing charges as it needs to search over all the possibilities (subcarrier combinations) within a

bandwidth. This is costly as it makes a joint search over all possibilities [16] and is impractical for large combination values due to its exponentially growing decoding complexity [15], which makes it unsuitable for WSN applications. Furthermore, the Log-Likelihood Ratio (LLR) detection strategy is another detection method proposed for this scheme for high number of subcarriers, but this detector may produce an undefined set of active indices not at all included in the original mapping table [15].

In this work, we introduce a modified frequency index modulation (FIM) scheme that is simpler than the approach of [15]. This system has a lower complexity compared to OFDM-IM, low power consumption profile and does not sacrifice data rate as it makes use of the frequency hops in a smart and wise way. As the proposed system does not use all of the available subcarriers, it will also enjoy inter-carrier interference-free transmission while it allows the transmission of additional bits in the index domain. Therefore, the proposed system is an excellent choice for WSNs.

In the proposed FIM scheme, the OFDM bandwidth is divided into equal N_B sub-bands of N subcarriers each. A message is divided into mapped and modulated blocks where the mapped block activates a single corresponding subcarrier in its predefined sub-band in order to carry the data content of the modulated block. At the receiver side, FFT is first performed on the received signal followed by sub-sectioning the bandwidth into N_B sub-bands where square-law envelope detector (SLED) is used in each sub-band to identify the active subcarrier. Then, the mapper chooses the corresponding indexed message and demodulates the received signal over the channel to get the remainder. The proposed system keeps the architecture simple and constitutes an excellent substitution for the conventional frequency-hopping (FH) technique in which hops carry no additional information. Despite the simplicity, the proposed system enjoys all the specifications associated with frequency hopping systems from the signal, interference, channel and anti-jamming points of view. Furthermore, the system has a low PAPR profile and may be used in multi-user or multi-node scenarios thanks to OFDMA multiple access technique. These properties make FIM scheme suitable for IoT applications where size, simplicity and efficiency say the final word [17].

In summary, the incomplex FIM system with its simple mapping method is briefly described. Analytical bit error rate (BER) expressions over Rayleigh fading channel are derived and are cross-checked with simulation results to show the accuracy extent of our analytical expressions. Further, the energy efficiency and PAPR of the proposed system are analysed. Finally, the BER performance of this scheme is compared with similar modulation techniques to show the FIM system superiority compared to its counterparts.

The rest of the paper can be summarized as follows. In Section II, the proposed system model is presented. Performance analysis of the FIM is demonstrated in Section III. Energy efficiency and complexity are discussed in IV.

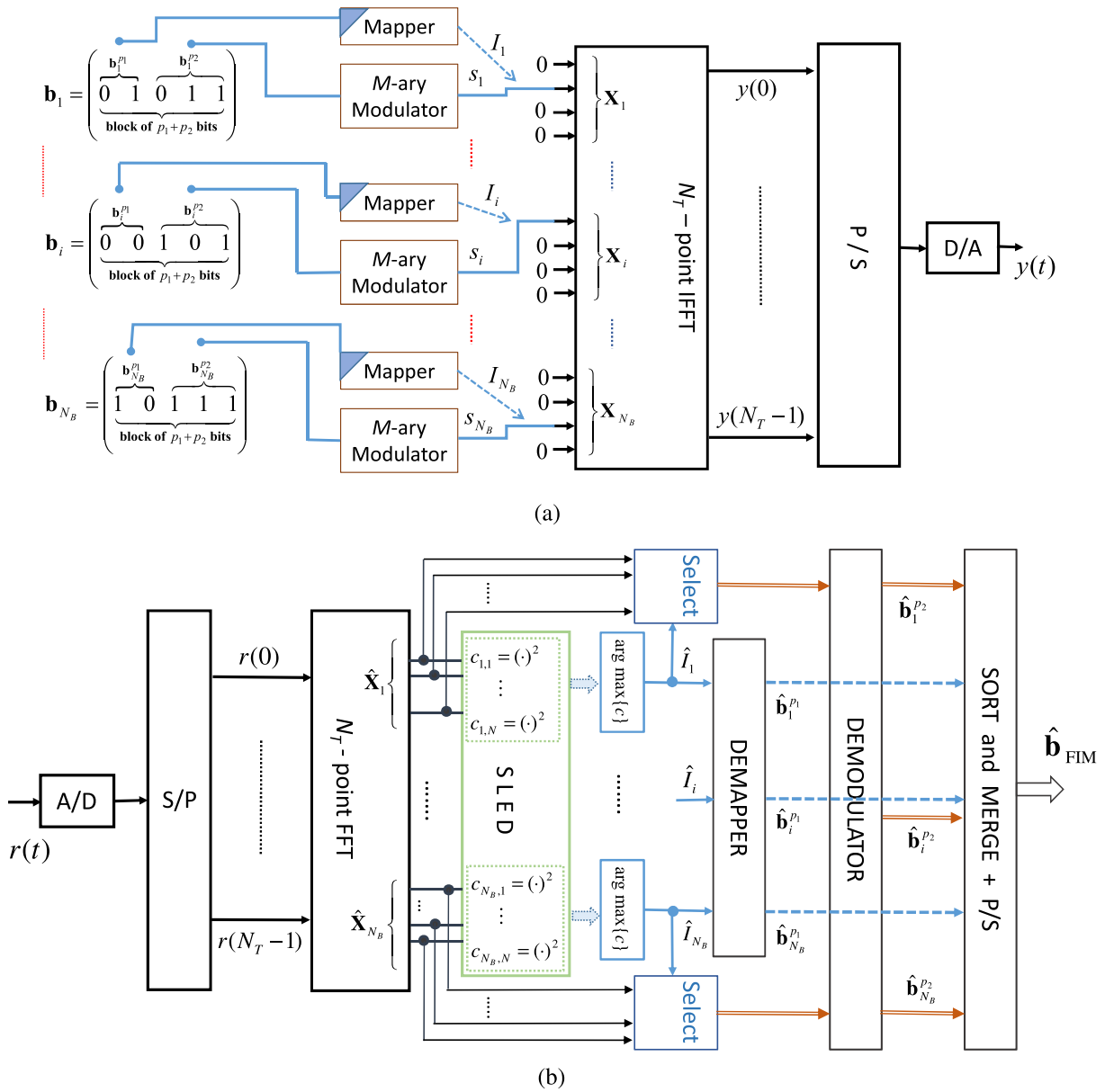


FIGURE 1. Block diagram of the general structure of FIM communication system. a) the transmitter, and b) the receiver.

In Section V, we present numerical and simulation results and Section VI provides concluding remarks.

II. SYSTEM MODEL

In this section, the FIM transmitter and the receiver architectures will be described in detail.

A. THE TRANSMITTER

A block diagram of the proposed FIM system is presented in Fig. 1. The FIM scheme divides the OFDM bandwidth of \$N_{FIM}\$ total sub carriers into \$N_B\$ equal sub-bands of \$N\$ subcarriers each. Since each FIM sub-block has the same processing procedure, we consider the \$i^{th}\$ sub-band for simplicity hereafter. In the FIM transmitter, the bit stream in every

sub-band is divided into blocks of \$p_n = p_1 + p_2\$ bits, where \$p_1\$ denotes the number of mapped bits while \$p_2\$ represents the number of modulated bits. As such, the outgoing bit stream can be written as \$\mathbf{b}_i = [\mathbf{b}_i^{p_1}, \mathbf{b}_i^{p_2}]\$, where \$\mathbf{b}_i \in \{0, 1\}^{(p_1+p_2)}\$, \$\mathbf{b}_i^{p_1} = [b_i^1, \dots, b_i^{p_1}]\$ and \$\mathbf{b}_i^{p_2} = [b_i^{p_1+1}, \dots, b_i^{p_2}]\$ are the two sub-blocks that represent \$p_1\$ mapped and \$p_2\$ modulated bits, respectively. Subsequently, the vector \$\mathbf{b}_i^{p_1} \in \{0, 1\}^{p_1}\$, of \$p_1 = \log_2(N)\$ bits, chooses one active subcarrier index \$I \in \{0, \dots, N - 1\}\$ out of \$N\$ available indices in the sub-band. The transformation of mapped bits into an active subcarrier index is performed by the index selector module. Fig. 2 illustrates the case where \$\mathbf{b}_i^{p_1} = [0 \ 1]\$ which leads to the activation of the second subcarrier, i.e. \$I_i = 2\$ out of 4 available subcarriers in the sub-band.

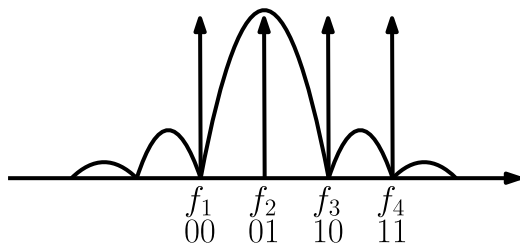


FIGURE 2. The frequency index transmission system with 4 subcarriers. In the illustration, the transmitter has indexed the message 01 and transmits the rest of the message via the subcarrier f_2 only.

On the other hand, the vector $\mathbf{b}_i^{p_2} \in \{0, 1\}^{p_2}$, of $p_2 = \log_2(M)$ bits, is mapped onto the considered M -ary signal constellation to produce the transmitted symbol s_i . The symbol s_i is transmitted over the selected subcarrier indexed by I_i , while the other $N - 1$ subcarriers are inactive and set to zero. The transmitted symbol s_i has an energy $E_s = E[s_i s_i^*] = p_2 E_b$ where E_b is the bit energy.

B. TOTAL MAPPED BITS p_T

Once the frequency modulation system with a total number of available frequencies N_{FIM} that is split into N_B number of sub-bands such that $N_{FIM} = N_B \times N$ is set up, the records shown in Table 1 may be discussed. In fact, Table 1 describes the total number of transmittable mapped bits $p_T = N_B \times p_1 = N_B \times \log_2(N)$ in the FIM system with respect to the number of sub-bands N_B for different N_{FIM} . Observe that the FIM system has a capacity to transmit a total of $N_B \times p_n$ bits in every transmission instant. Since both the peak power in the system as well as the BER performance depend on the number of active frequencies in a sub-band, Table 1 will be revisited again later, when we discuss PAPR analysis and simulation results in the sections that follow.

Also, since some parts of the transmitted bits are conveyed by the frequency index, and in order to have a fair comparison with other conventional systems, we define an equivalent system bit energy E_{bs} which represents the effective energy consumed per transmitted bit. This equivalent system bit energy is related to the physically modulated bit energy by the relationship

$$E_{bs} = \frac{p_1 + p_2}{p_2} E_b = \frac{p_n}{p_2} E_b. \tag{1}$$

While the energy described in (1) allows the comparison of our system to other systems from the performance point of view, it also is an indication of the energy efficiency achieved by the proposed system. Furthermore, to construct the FIM sub-block of N elements in the frequency domain, we consider the selected active subcarrier index I_i and the modulated M -PSK symbol s_i , in order to form the vector

$$\mathbf{X}_i = [X_i(0), \dots, X_i(N - 1)], \tag{2}$$

TABLE 1. FIM transmits a total of p_T mapped bits using N_B number of sub-bands with N frequencies each.

N_{FIM}	4	8	16	32	64	128	256
N_B	2	2	2	2	2	2	2
N	2	4	8	16	32	64	128
p_T	2	4	6	8	10	12	14
N_B		4	4	4	4	4	4
N		2	4	8	16	32	64
p_T		4	8	12	16	20	24
N_B			8	8	8	8	8
N			2	4	8	16	32
p_T			8	16	24	32	40
N_B				16	16	16	16
N				2	4	8	16
p_T				16	32	48	64
N_B					32	32	32
N					2	4	8
p_T					32	64	96
N_B						64	64
N						2	4
p_T						64	128
N_B							128
N							2
p_T							128

where

$$X_i(k) = \begin{cases} 0, & k \neq I, \\ s_i, & k = I, \text{ for } k = 0, \dots, N - 1. \end{cases} \tag{3}$$

For simplicity, the insertion and removal of cyclic guard prefix is not expressed in our mathematical equations.

The frequency index modulators in each sub-band of the transmitter obtain the FIM subblocks first and then concatenate these subblocks to form the main FIM blocks. So, the complete FIM transmitted block that incorporates all sub-bands (from 1 until N_B) would be stated as

$$y(t) = \frac{1}{\sqrt{T_N}} \sum_{i=1}^{N_B} \sum_{k=0}^{N-1} X_i(k) e^{j2\pi f_{i,k} t}, \quad 0 \leq t \leq T_N, \tag{4}$$

where $f_{i,k}$ is the k^{th} subcarrier frequency in the i^{th} sub-band with a predefined bandwidth of $f_{i,k} = N(i - 1)/T_N + k/T_N$ with T_N being the time duration of a FIM symbol.

C. THE RECEIVER

In this paper, we consider transmissions over a Rayleigh fading channel corrupted by an additive Gaussian noise channel. The received signal in the i^{th} sub-block can be expressed as a vector of N samples $\hat{\mathbf{X}}_i = [\hat{X}_i(0), \dots, \hat{X}_i(N)]$ such that

$$\hat{X}_i(k) = \begin{cases} Z'_i, & k \neq I, \\ H_i s_i + Z_i, & k = I, \text{ for } k = 0, \dots, N - 1. \end{cases} \tag{5}$$

where $H_i \sim \mathcal{CN}(0, 1)$ is the FFT output produced by the Rayleigh fading channel effect, Z'_i and Z_i are independent complex AWGN, with zero mean and variance N_0 . In order

to reduce the complexity of the receiver, a SLED is used to estimate the active subcarrier index in the i^{th} sub-block. Thus, the output variables in the vector $\hat{\mathbf{X}}_i$ are fed to SLED forming N decision variables such that for $k = 0, \dots, N - 1$, we have

$$c_{i,k} = |\hat{X}_i(k)|^2 = \begin{cases} |Z_i'|^2, & \mathcal{H}_0 \\ |H_i s_i + Z_i|^2, & \mathcal{H}_1 \end{cases} \quad (6)$$

where \mathcal{H}_0 and \mathcal{H}_1 are two hypotheses with which \mathcal{H}_0 is verified if there is no signal, and \mathcal{H}_1 is the alternative that indicates the presence of s_i . The SLED chooses the maximum value in order to estimate the active subcarrier index, such that the estimate of the active subcarrier index would be expressed as

$$\hat{I}_i = \arg \max_k \{c_{i,k}\}, \quad k \in \{0, \dots, N - 1\}. \quad (7)$$

Therefore, the decision variable might land in \mathcal{H}_1 if $\hat{I}_i = I_i$. By estimating the active subcarrier index \hat{I}_i , the receiver extracts p_1 mapped bits. The receiver then demodulates the corresponding branch output using a conventional M -PSK demodulator to extract the remaining p_2 modulated bits.

III. FIM PERFORMANCE ANALYSIS

In this section, we determine the performance of the proposed FIM system, in order to examine the advantages of mapping information bits into subcarrier indices.

A. BER ANALYSIS OF FIM

In the FIM scheme, the transmitted data in every sub-band is divided into two blocks; the *mapped bits* block and the *modulated bits* block. The mapped bits block determines which subcarrier will be active and, hence, will be modulated by the modulating bits contained in the *modulated bits* block. Therefore, the FIM system BER probability consists of the BER probability of mapped bits P_{map} and the BER probability of modulated bits P_{mod} . Subsequently, the FIM BER could be described as

$$P_{\text{FIM}} = \frac{p_1}{p_1 + p_2} P_{\text{map}} + \frac{p_2}{p_1 + p_2} P_{\text{mod}}. \quad (8)$$

In (8) above, the probability of error is prorated to the number of bits in every category and the errors committed in that category. In order to derive the BER probability of mapped bits P_{map} , the erroneous probability of active subcarrier index detection P_{ed} should be derived. Erroneous active subcarrier index detection causes a wrong mapped bits combination estimation. Each wrong combination can have a different number of incorrect bits compared to the correct combination. Therefore, the probability of erroneous active subcarrier index detection is converted into the corresponding BER probability of mapped bits by using

$$P_{\text{map}} = \frac{2^{(p_1-1)}}{2^{p_1} - 1} P_{\text{ed}}. \quad (9)$$

In order to calculate the BER of the modulated bits P_{mod} , we consider the fact that this probability depends on the correct estimation of the active subcarrier index and the BER

probability of M -ary PSK modulation. Therefore, an error may occur in two different ways. The first case is when the active subcarrier index is correctly estimated but an error occurs in the M -PSK demodulation process. The second case is when an error occurs in the estimation of the active subcarrier index, and the modulated bits are estimated using the wrong subcarrier. In this case, the M -PSK modulated symbol will have to be guessed. In fact, the probability of correct detection will be simply equal to $\frac{1}{M}$. Consequently, the BER probability of the modulated bits would be expressed as

$$P_{\text{mod}} = \frac{1}{p_2} \left[P_{S,\text{MPSK}}(1 - P_{\text{ed}}) + \frac{M-1}{M} P_{\text{ed}} \right], \quad (10)$$

where $P_{S,\text{MPSK}}$ is the conventional SER probability of M -PSK modulation. As both (9) and (10) in the above depend on P_{ed} , we have a detailed look at this probability in the next subsection.

B. PROBABILITY OF ERRONEOUS ACTIVE SUBCARRIER INDEX DETECTION P_{ed}

Since a SLED is used for active subcarrier index estimation, we shall determine the probability of erroneous active subcarrier index detection P_{ed} . To do so, we assume equiprobable transmitting active subcarriers. Moreover, for the sake of clarity, we focus on a single sub-band, i.e the i^{th} sub-band, in which $c_{i,k}$ in (6) becomes c_k for $k = 0, \dots, N - 1$. Therefore, P_{ed} the probability of error conditioned on the transmitting subcarrier index being $I \in \{0 \dots N - 1\}$ would be given as

$$P_{\text{ed}} = P(c_I < \max_{k \neq I} (c_k) | I), \quad \text{for } 0 \leq k \leq N - 1. \quad (11)$$

As deduced from (11), an error in the estimation of the active subcarrier index will occur if the decision variable $\max(c_k)$ is larger than c_I . It can be observed from (6) that the variable c_k may assume two values as

$$c_k = \begin{cases} |Hs + Z_I|^2, & k = I, \\ |Z_k|^2, & k \neq I. \end{cases} \quad (12)$$

Since the complex-valued random variables $\{Hs\}$, $\{Z_I\}$ and $\{Z_k\}$ are mutually independent zero mean Gaussian random variables, the decision variables c_I and c_k are distributed according to a chi-square distribution with two degrees of freedom. Subsequently, its probability density functions (PDF) can be written as

$$p(c_I) = \frac{1}{2\sigma_I^2} e^{-c_I/2\sigma_I^2}, \quad (13)$$

where the variance σ_I^2 is given by

$$\begin{aligned} \sigma_I^2 &= \mathbb{E} \left(|Hs + Z_I|^2 \right) \\ &= \mathbb{E} \left((Hs + Z_I) (Hs + Z_I)^* \right) \\ &= \mathbb{E}(|H^2|)E_s + N_0 = N_0(1 + \bar{\gamma}_s), \end{aligned} \quad (14)$$

where $\bar{\gamma}_s = \mathbb{E}(|H|^2)E_s/N_0$ is the average signal-to-noise ratio (SNR). Since the usual metrics for BER performance

analysis in digital communications is the E_b/N_0 , the expression (14) can be rewritten as

$$\sigma_I^2 = N_0(1 + p_2\bar{\gamma}_b), \quad (15)$$

where $\bar{\gamma}_b = \mathbb{E}(|H|^2)E_b/N_0$. Similarly, for $k \neq I$, the variance σ_k^2 is calculated based on the PDF

$$p(c_k) = \frac{1}{2\sigma_k^2} e^{-c_k/2\sigma_k^2} \quad (16)$$

that results in

$$\sigma_k^2 = \mathbb{E}(|Z_k|^2) = N_0, \quad \text{for } 0 \leq k \leq N-1, \quad k \neq I. \quad (17)$$

The probability of erroneous active subcarrier index estimation is equal to 1 minus the probability that $c_I > c_k$, for $0 \leq k \leq N-1$. Since the signals are orthogonal and the AWGN are statistically independent, the random variables in (12) are mutually statistically independent. Hence, for a given I the joint probability $P(\{c_I > c_k\}|I)$, for $0 \leq k \leq N-1$ is equal to $P(c_I > c_k|I)$, for $k \neq I$, raised to the $N-1$ st power. Furthermore, we may now evaluate the probability $P(c_I > c_k|I)$ by applying

$$P(c_I > c_k|I) = \int_0^{c_I} p(c_k) dc_k. \quad (18)$$

The evaluation of the above integral results in [18]

$$P(c_I > c_k|I) = 1 - e^{-\frac{c_I}{2\sigma_k^2}}. \quad (19)$$

Raising the result of (19) to the power $N-1$ and averaging over all possible values of c_I will yield the probability of correct decision P_{cd} .

$$P_{cd} = \int_0^\infty p(c_I) \left[1 - e^{-\frac{c_I}{2\sigma_k^2}} \right]^{N-1} dc_I. \quad (20)$$

Since $p(c_I)$ as been defined in (13), we get

$$\begin{aligned} P_{cd} &= \int_0^\infty \frac{1}{2\sigma_I^2} e^{-\frac{c_I}{2\sigma_I^2}} \left[1 - e^{-\frac{c_I}{2\sigma_k^2}} \right]^{N-1} dc_I \\ &= \int_0^\infty \frac{1}{1 + p_2\bar{\gamma}_b} e^{-\frac{c_I}{1+p_2\bar{\gamma}_b}} \left[1 - e^{-c_I} \right]^{N-1} dc_I, \end{aligned} \quad (21)$$

Note that the term $[1 - e^{-c_I}]^{N-1}$ which appears in (21) may be expressed in a reduced form as

$$[1 - e^{-c_I}]^{N-1} = \sum_{k=0}^{N-1} (-1)^k \binom{N-1}{k} e^{-kc_I}. \quad (22)$$

Now, substituting (22) into (21), we get [18]

$$\begin{aligned} P_{cd} &= \frac{1}{1 + p_2\bar{\gamma}_b} \sum_{k=0}^{N-1} (-1)^k \binom{N-1}{k} \\ &\quad \times \int_0^\infty e^{-\frac{c_I}{1+p_2\bar{\gamma}_b}} e^{-kc_I} dc_I. \end{aligned} \quad (23)$$

Unifying the exponential terms in the integral produces

$$\begin{aligned} P_{cd} &= \frac{1}{1 + p_2\bar{\gamma}_b} \sum_{k=0}^{N-1} (-1)^k \binom{N-1}{k} \\ &\quad \times \int_0^\infty e^{-\frac{(1+k+p_2\bar{\gamma}_b)c_I}{1+p_2\bar{\gamma}_b}} dc_I. \end{aligned} \quad (24)$$

Replacing the integral term by its solution yields

$$P_{cd} = \frac{1}{1 + p_2\bar{\gamma}_b} \sum_{k=0}^{N-1} (-1)^k \binom{N-1}{k} \left[\frac{1 + p_2\bar{\gamma}_b}{(1 + k + kp_2\bar{\gamma}_b)} \right], \quad (25)$$

which then simplifies to the final form of

$$P_{cd} = \sum_{k=0}^{N-1} \frac{(-1)^k}{1 + k + kp_2\bar{\gamma}_b} \binom{N-1}{k}. \quad (26)$$

Subtracting the above result from unity gives the probability of subcarrier detection error, or the mapped symbol error i.e. $P_{ed} = 1 - P_{cd}$ as

$$P_{ed} = 1 - P_{cd} = \sum_{k=1}^{N-1} \frac{(-1)^{1+k}}{1 + k + kp_2\bar{\gamma}_b} \binom{N-1}{k}. \quad (27)$$

C. BER OF MAPPED AND MODULATED BITS

Once the probability of subcarrier misdetection P_{ed} is evaluated as in (27), it is substituted in (9) and (10) to yield the BER of mapped and modulated bits, respectively. In the latter, the conventional M -PSK demodulation with the following closed-form SER expression over fading channels is considered [18]

$$P_{S,MPSK} = \frac{M-1}{M} - \frac{V}{\pi\sqrt{1-W^2}} \cot^{-1} \left(\frac{-W}{\sqrt{1-W^2}} \right), \quad (28)$$

where $V = \mu \sin(\pi/M)$, $W = \mu \cos(\pi/M)$ and μ is given as

$$\mu = \sqrt{\frac{p_2\bar{\gamma}_b}{1 + p_2\bar{\gamma}_b}}. \quad (29)$$

Substituting (27) and (28) into (9) and (10) respectively, and considering the expression for the probability of error for FIM systems introduced in (8), we end up with the final expanded form as shown on the top of the next page.

IV. ENERGY EFFICIENCY, PAPR AND COMPLEXITY

In this section, we consider the energy efficiency, PAPR and complexity analyses for the proposed FIM system.

A. ENERGY EFFICIENCY

Table 1 demonstrates various possible configurations for a given total number of subcarriers N_{FIM} . We observe that when N_{FIM} increases, we have more design options. In fact, we have $\log_2(N_{FIM}/2)$ possible configurations, where for each configuration, different number of bits are mapped. In the table, values of N_{FIM} from 4 to 256 are shown. As clearly observed in Table 1, the maximum number of mapped bits in a FIM

$$P_{\text{FIM}} = \frac{1}{p_n} \left[\left(\frac{M-1}{M} - \frac{\sqrt{\frac{p_2 \bar{\gamma}_b}{1+p_2 \bar{\gamma}_b}} \sin(\pi/M)}{\pi \sqrt{1 - \left(\sqrt{\frac{p_2 \bar{\gamma}_b}{1+p_2 \bar{\gamma}_b}} \cos(\pi/M)\right)^2}} \cot^{-1} \left(\frac{-\sqrt{\frac{p_2 \bar{\gamma}_b}{1+p_2 \bar{\gamma}_b}} \cos(\pi/M)}{\sqrt{1 - \left(\sqrt{\frac{p_2 \bar{\gamma}_b}{1+p_2 \bar{\gamma}_b}} \cos(\pi/M)\right)^2}} \right) \right) \sum_{k=0}^{N-1} \frac{(-1)^k}{1+k+k p_2 \bar{\gamma}_b} \binom{N-1}{k} \right. \\ \left. + \frac{M-1}{M} \sum_{k=1}^{N-1} \frac{(-1)^{1+k}}{1+k+k p_2 \bar{\gamma}_b} \binom{N-1}{k} \right] + \frac{p_1}{p_n} \frac{2^{(p_1-1)}}{2^{p_1}-1} \sum_{k=1}^{N-1} \frac{(-1)^{1+k}}{1+k+k p_2 \bar{\gamma}_b} \binom{N-1}{k} \quad (30)$$

TABLE 2. Comparison, OFDM, OFDM-IM and FIM systems for the conveyance of 3 bits per transmission.

	OFDM	OFDM-IM(4,2)	FIM $M = 2, N = 4$
Complexity	22	28	22
Energy saving	0%	33.3%	66.6%

system with a total of N_{FIM} frequencies is equal to $p_T = N_{\text{FIM}}/2$. This maximum mapping is achieved in two ways, choosing N either 2 or 4. That is to say, to divide N_{FIM} into sub-bands such that we have either 2 or 4 frequencies in each sub-band. Choosing $N = 2$ halves the transmitted power, but it does not render a BER performance improvement over the basic system. However, choosing $N = 4$ not only provides a lower PAPR and a better power efficiency compared to $N = 2$, as only 1 out of 4 frequencies becomes active, but achieves a BER enhancement and allows the system to carry an extra mapped bit compared to the $N = 2$ case.

In the proposed FIM only $N_B p_2$ bits from the total $N_B(p_1 + p_2)$ are directly modulated using the M -ary modulation, whereas $N_B p_1$ bits are conveyed in the selection of subcarriers. Considering that each modulated bit requires an energy of E_b to be transmitted, then the mapping part to index subcarriers should reduce the total required transmission energy. Consequently, the percentage of the energy saving per sub-band in the proposed FIM is given by

$$E_{\text{saving}} = \left(1 - \frac{p_2}{p_1 + p_2} \right) E_b \% \\ = \left(1 - \frac{1}{p_1/p_2 + 1} \right) E_b \% \quad (31)$$

Since we have defined $p_1 = \log_2(N)$ and $p_2 = \log_2(M)$, the energy saving depends on the ratio of the number of subcarriers involved in indexing to the modulation order of the system. It should be noted that for a fixed modulation order, an augmentation in the number of subcarriers to be indexed yields more energy saving in the FIM system. Table 2 at the end of Section V provides a numerical example in relation to the energy saving discussed here.

B. PAPR ANALYSIS

Taking into consideration the splitting of a full band that encompasses N_{FIM} frequencies into N_B sub-bands with N frequencies each, we will have a glance at the PAPR behaviour of the proposed system. The PAPR is a criterion to measure the success of a frequency modulation system and is defined

in OFDM systems for a transmit signal $y(t)$ as [19]

$$\text{PAPR}_{\text{dB}} = 10 \log_{10} \frac{\max |y(t)|^2}{E\{|y(t)|^2\}} \quad (32)$$

to represent an indication of the non-linearity in the transmitter amplifier. PAPR is ideally required to stay within the linear operational range of the RF amplifier at the transmitter. Assuming that the real and imaginary parts of $y(t)$ follow a Gaussian distribution, each with zero mean and variance $\frac{1}{2}$ in agreement with the central limit theorem, when N_{FIM} is sufficiently large, $|y(t)|$ becomes a Rayleigh distribution and the power distribution has central chi-square distribution with two degrees of freedom [20]. The cumulative distribution function (CDF) of the amplitude of a signal sample is given by

$$F(\text{PAPR}_0) = 1 - e^{-\text{PAPR}_0}. \quad (33)$$

If we assume that the average power of $y(t)$ is equal to one, then the sampling values of different sub-channels are mutually independent and identically distributed Rayleigh random variables normalized with its own average power. Hence, the probability distribution function for PAPR being less than a certain threshold value becomes

$$\Pr(\text{PAPR} \leq \text{PAPR}_0) = F(\text{PAPR}_0)^{N_B} \\ = (1 - e^{-\text{PAPR}_0})^{N_B}. \quad (34)$$

However, when the performance for PAPR reduction techniques need to be evaluated, the complementary cumulative distribution function (CCDF) of the PAPR is more frequently used [21], *i.e.* the probability that PAPR exceeds a predefined threshold value PAPR_0 , such that

$$\Pr(\text{PAPR} > \text{PAPR}_0) = 1 - \Pr(\text{PAPR} \leq \text{PAPR}_0) \\ = 1 - F(\text{PAPR}_0)^{N_B} \\ = 1 - (1 - e^{-\text{PAPR}_0})^{N_B}. \quad (35)$$

The partial selection of the subcarriers in FIM results in a reduction of the PAPR. Such a PAPR reduction considerably decreases the consumed power and is not associated with any form of penalty on the bit error rate (BER) performance.

C. SYSTEM COMPLEXITY

The complexity of the FIM system can be evaluated by the number of operations required. Since the FIM uses IFFT and FFT operations with a length of N_{FIM} , the computational complexity will be $\mathcal{O}_{\text{FFT/IFFT}} \sim \mathcal{O}(2N_{\text{FIM}} \log_2(N_{\text{FIM}}))$. Next,

SLED multiplies the vector $\hat{\mathbf{X}}_i$ by its complex conjugate. Therefore, the computational complexity is simply $\mathcal{O}_{\text{SLED}} \sim \mathcal{O}(NN_B)$. Regarding the modulation and the demodulation, we assume that a modulator converts a stream of p_2 bits into an M -ary symbol by computing an inner product between the bit stream and the vector $[2^{p_2-1}, \dots, 1]$. The demodulator will convert the symbol into a bit stream by computing p_2 Euclidean divisions. As a result, the computational complexity of a modulator and a demodulator will be $\mathcal{O}_{\text{Mod/Demod}} \sim \mathcal{O}(3p_2 - 1)$ per active subcarrier. In total, the complexity of the FIM system would be expressed as

$$\mathcal{O}_{\text{FIM}} = \mathcal{O}_{\text{FFT/IFFT}} + \mathcal{O}_{\text{SLED}} + N_B \mathcal{O}_{\text{Mod/Demod}}. \quad (36)$$

In the conventional OFDM scheme, since all subcarriers are activated during the transmission, the complexity will be

$$\mathcal{O}_{\text{OFDM}} = \mathcal{O}_{\text{FFT/IFFT}} + NN_B \mathcal{O}_{\text{Mod/Demod}}. \quad (37)$$

Aiming at comparing the FIM system to a system that shares the same modulation concept but with a different receiver design, we compare the complexity of FIM to that of OFDM-IM. In the latter, only k out of N subcarriers are activated. However, the complexity of the maximum likelihood detector is $\mathcal{O}_{\text{MLD}} \sim \mathcal{O}(2^{p_2 M^k})$ per subcarrier where $k = p_2 / \log_2(M)$, [15].

$$\mathcal{O}_{\text{OFDM-IM}} = \mathcal{O}_{\text{FFT/IFFT}} + kN_B \mathcal{O}_{\text{Mod/Demod}} + \mathcal{O}_{\text{MLD}}. \quad (38)$$

V. SIMULATION RESULTS

In this section, we study the obtained analytical and simulation results for the proposed FIM system and show that analytical and simulation results are in good agreement. Then we compare the performance of FIM to other index-based schemes like SM and OFDM-IM system. Finally, we study the energy efficiency, PAPR and complexity analyses for the proposed system.

A. PERFORMANCE OF FIM

We shed light in this section on some of the parameters that influence the system the most, we investigate the performance of the proposed frequency-index modulation system in various scenarios and we compare the performance of our system to other modulation-index schemes to show the performance superiority.

As the system may ferry a certain number of symbols per sub-band in every transmission using various configurations, we start by plotting the overall BER performance of the FIM system described by (8) for the transmission of 7 bits per sub-band using different combinations of the modulation order M and the number of frequencies per sub-band N . The performance of such a case is shown in Fig. 3. The first observation is that all configurations of the FIM system show a superior BER performance to the conventional 128-ary PSK modulation in fading channels. As a matter of fact, the 128-ary PSK has been chosen to compare, as it represents the most basic well-known communication system that carries 7 bits. We also observe a great match and conformity between

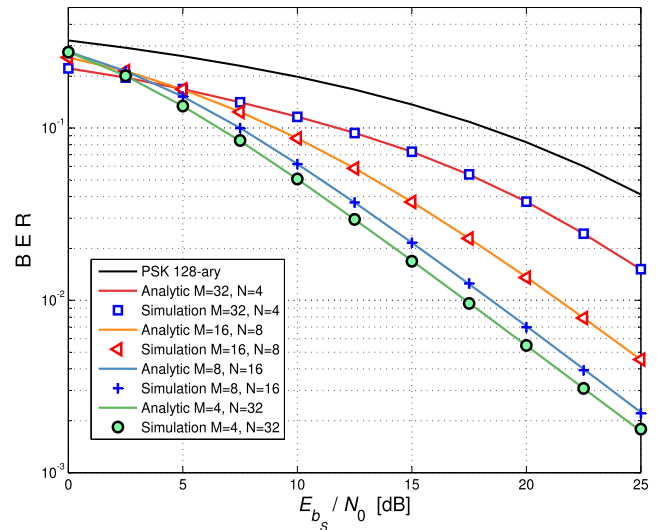


FIGURE 3. Performance of the proposed system with various values of M and N that facilitate the conveyance of 7 bits per transmission.

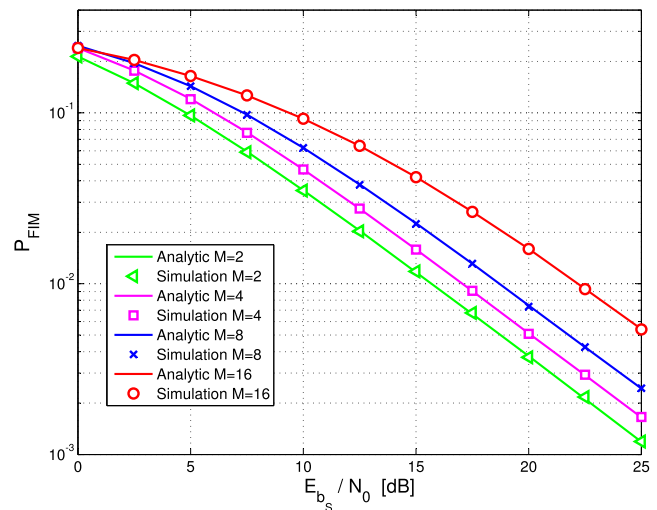


FIGURE 4. Performance of the proposed FIM system with various modulation order M for $N = 4$ subcarriers per sub-band.

analytical and simulation results for the FIM system, which confirms the certitude of our approach. Furthermore, Fig. 3 shows that under transmission rate restrictions, our system is design-flexible and is adaptable to acquire several forms in terms of M and N . This facilitates its practical application for WSNs. As both the modulation order M and the number of frequencies per sub-band N constitute the fundamental parts of the FIM design, we independently observe the BER performance of FIM with respect to each of these parameters individually in the next two plots. Fig. 4 shows the BER performance of the proposed FIM system versus the modulation order M , for $N = 4$ frequencies per sub-band. As seen in Fig. 4, increasing M tightens up the Euclidean distance between the transmitted symbols and degrades the BER performance, which is very well in line with communication theory. Fig. 5 exhibits the BER performance of the proposed FIM system with respect to the number of subcarriers per sub-band for a modulation order of $M = 8$. As witnessed

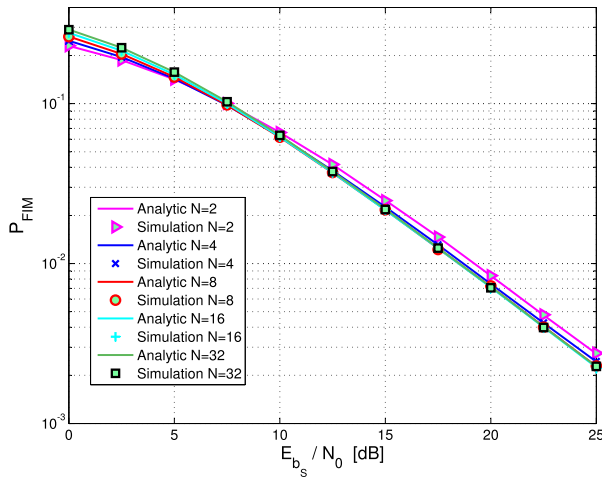


FIGURE 5. Performance of the proposed FIM system for various subcarriers per sub-band and a modulation order of $M = 8$.

in Fig. 5, the BER performance of the proposed system shows a marginal improvement with increased N . This is due to the fact that increasing N contributes to the total equivalent system bit energy described earlier in (1). As a matter of fact, the BER performance would deteriorate without the contribution of the energy contained in the mapped bits, because increasing N challenges the receiver to choose a correct sub-carrier from within a larger set and, therefore, deteriorates the BER performance. However the energy contribution made by the mapped bits balances the performance. This figure affirms that the only price paid for conveying more mapped bits as N gets larger is bandwidth expansion, not BER performance alteration.

B. PERFORMANCE COMPARISON WITH SM AND OFDM-IM SYSTEMS

To exhibit the supremacy of the frequency index-modulation system despite its simplicity, we compare the performance of our proposed work to the performance of two other index-modulation based schemes, namely the spatial modulation (SM) and the orthogonal frequency division multiplexing with index modulation (OFDM-IM) techniques. These two works are very well explained in [4]–[7] and [15]. For simplicity, we consider a comparison with SM and OFDM-IM for the case of dispatching 3 bits per transmission. In this case, the modulation order of SM is set to $M = 4$, while the number of transmitting antennae is fixed at $N_t = 2$ transmitting antennae versus a single receiving antenna, i.e. $N_r = 1$. We have chosen this case for SM as it shows a better performance compared to the other way round, e.g. $N_t = 4$ and $M = 2$. Furthermore, the OFDM-IM system has 4 subcarriers in each sub-band, where 2 subcarriers are active. All the three systems considered for comparison here are simulated under similar channel and fading conditions. In order to have a fair comparison in terms of energy with respect to SM, the energy of SM has been reformulated in a fashion similar to (1) such that it incorporates the energy of the mapped bits too, i.e. $E_{b_{SM}} = \frac{\log_2(N_t) + \log_2(M)}{\log_2(M)} \cdot E_{b_{SM0}}$ where

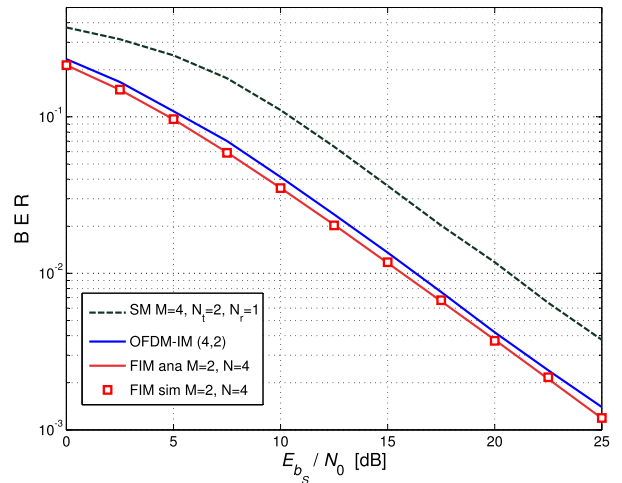


FIGURE 6. Performance of FIM in comparison to SM and OFDM-IM technologies, for the transmission of 3 total bits (mapped and modulated).

$E_{b_{SM0}}$ is the default energy of the SM system. As depicted in Fig. 6, the FIM system achieves a noticeable performance despite its simplicity and ease. The performance of the proposed FIM system is in tight competition with OFDM-IM. It is of course possible to enhance the performance of any of these index-modulation schemes by implementing more receiver antennae and increasing reception diversity, however this is absolutely impractical for wireless sensor cases, where size and simplicity are of extreme importance.

Indeed, the admirable advantage of the proposed system lies in its simplicity and suitability for application in WSNs. Unlike SM that requires expensive and bulky hardware with a performance totally antenna- and channel gain-dependent, and unlike OFDM-IM that is too complex for WSNs implementation. Furthermore, both SM and OFDM-IM are ML-detector dependent, the implementation of which becomes impractical for large combinations of M and N . In addition, neither SM nor OFDM-IM may function without the availability of perfect channel state information at the receiver. In the proposed FIM scheme, however, the performance is achieved without undergoing any expensive hardware expansion or complex algorithmic implementation. Added that the proposed scheme may very well convey p_1 bits per transmission and detect them using the SLED, without having any knowledge of the channel state information at all. This is absolutely not possible, neither with SM nor with OFDM-IM.

C. ENERGY EFFICIENCY, PAPR AND COMPLEXITY ANALYSIS

In this subsection, we show the results concerning energy efficiency, PAPR and complexity analyses in 3 different consecutive and independent clauses for sake of clarity.

1) ENERGY EFFICIENCY AND PAPR ANALYSIS

We compare the CCDF of the PAPR in terms of number of sub-bands N_B . This is because a single subcarrier is activated

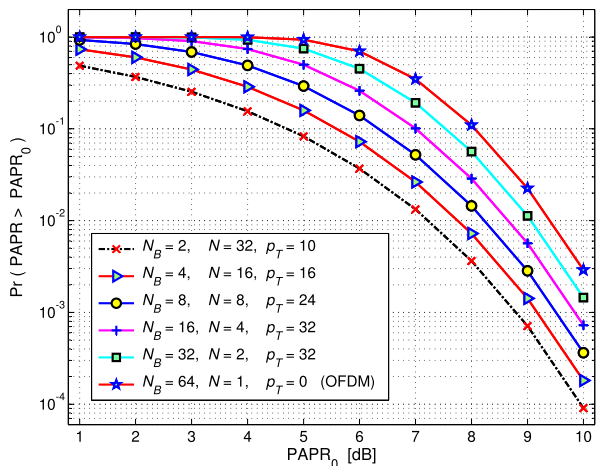


FIGURE 7. CCDFs of the PAPR of the proposed FIM system with complementing N_B and N combinations for $N_{FIM} = 64$.

in every sub-band, and in effect, only N_B subcarriers are active per every FIM transmission. Fig. 7 shows the theoretical CCDFs of the proposed FIM system with different sub-bands for $N_{FIM} = 64$ based on evaluating (35). Notice that the case $N_B = 64, N = 1$ in Fig. 7 corresponds to the PAPR of a conventional OFDM system with 64 subcarriers, where no frequency-indexing takes place. As clearly illustrated in Fig. 7, increasing the number of subcarriers per sub-band N leads to lesser N_B which in turn causes the CCDF to diminish. It is observed here that the FIM system transmits fewer p_T bits and relaxes the PAPR for higher N and less N_B . Conversely, more p_T bits are transmitted for higher N_B and less N at the cost of higher PAPR values.

High PAPR can be avoided by reducing the number of subcarriers actually engaged in transmission, and in effect, the PAPR is reduced in a fashion similar to clustered OFDM [22], [23]. Note that in the clustered OFDM technique mentioned in [22] and [23] the subcarriers are clustered into several smaller blocks and transmitted over separate antennae. The PAPR is reduced since there are fewer subcarriers per transmission. But that technique has not been widely employed since the increase in the number of power amplifiers makes their proposal impractical in many applications. However, in our work, we have a single antenna and the implementation of several antennae has been substituted by using a frequency-indexing method. Brief, we reduce PAPR by clustering using various frequency bands instead, to replace the deployment of several antennae.

Regarding the energy efficiency, the proposed FIM system the energy saving is significant as the number of mapped bits increases (see (31)). Compared to FH or OFDM systems, the FIM system is competitive in terms of energy efficiency for a given number of bits per transmission. Instead of using a pseudo-random generator to select a frequency as in FH, FIM activates one subcarrier which is selected by the mapper (the index selector). As a result, if $p_n = p_1 + p_2$ bits need to be transmitted, FH systems will use $E_{FH} = p_n E_b$ whereas FIM system will dispose $E_{FIM} = p_2 E_b$, where E_b is the

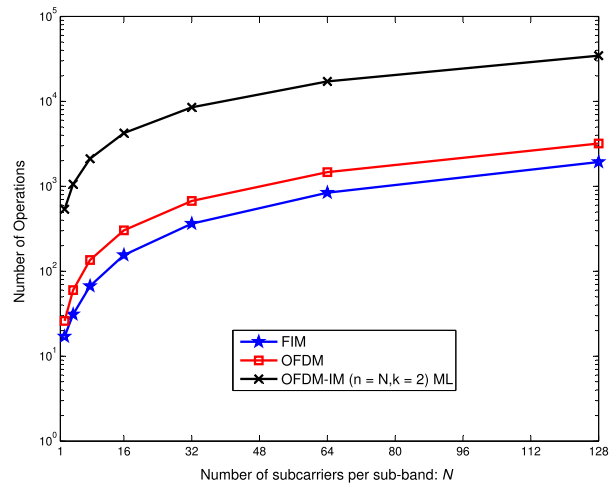


FIGURE 8. Complexity comparison of the proposed FIM, conventional OFDM and OFDM-IM(n,k) systems using a single sub-band $N_B = 1$ and FFT-length $N_{FIM} = NN_B$.

energy to transmit one bit. For example, for $p_n = 2$ bits per transmission, it is possible to use one bit for index mapping and another bit for modulation in the FIM system whereas both bits will be transmitted via the activation of various hoppings in the FH. Under this condition, from (31), FIM will save 50% of energy compared to conventional FH. It can be seen that the percentage of energy saving will be reduced as the modulation order increases, i.e as $p_2 \rightarrow \infty$.

2) SYSTEM COMPLEXITY

The computational complexity of these systems is considered for evaluation here. We compare the complexity of FIM to that of conventional OFDM, by fixing the the modulation order. As such, we observe that the complexity of the OFDM pertaining to modulation and demodulation parts is $\sim 3N \log_2(M)$ whereas the complexity of the FIM scheme is $\sim N + 3 \log_2(M)$. Clearly, as the number of subcarriers increases, $N > 1$, the FIM scheme wins in terms of low-complexity. Furthermore, since the OFDM-IM uses the maximum likelihood detection, its computational complexity is higher than the others. In fact we have $\mathcal{O}_{FIM} \leq \mathcal{O}_{OFDM} \leq \mathcal{O}_{OFDM-IM}$. Fig. 8 depicts the computational complexity based on (36), (37) and (38) that represent the complexity of these OFDM-like systems, by fixing the modulation order to a 16-PSK modulation. It is clearly observed that higher number of active subcarriers involved in transmission increases the computational complexity, and that FIM has the lowest complexity compared to others.

However, the number of bits per transmission will not be the same in these systems. Indeed, if one single subcarrier is activated per transmission, then the number of bits per transmission will be $p_{nFIM} = \log_2(M) + \log_2(N)$ whereas $p_{nOFDM} = N \log_2(M)$ in the conventional OFDM system because every subcarrier is activated. For the OFDM-IM, the number of bits per transmission is $p_{nOFDM-IM} = k \log_2(M) + \log_2(N)$. Clearly, the FIM scheme has the lowest number of bits per transmission. Table 2 depicts the performance of these

systems for the conveyance of 3 bits per transmission. In this case, the complexity of the FIM is comparable to the OFDM but we have 66.6% of energy saving. The OFDM-IM saves only 33.3% of the energy and have the highest complexity due to the maximum likelihood decoder. In this condition, the proposed FIM system is competitive to the current state of the art in terms of energy saving and complexity. This renders the proposed system exceptionally adaptable to WSN applications.

VI. CONCLUSIONS

In this paper, we have proposed a frequency-index modulation (FIM) scheme that suits the physical layer of IoT applications. The proposed system uses OFDM waveforms for its ease of implementation and flexibility. Unlike SM and OFDM-IM which are either hardware-demanding or too complex to be implemented based on the *index modulation* technique, the suggested system conveys addition information bits by virtue of the active frequency indices in every sub-band. At the modulator side, the bit stream is divided into two blocks: mapped and modulated. The bits within the mapped block are used to activate the corresponding subcarrier to carry the data content of the modulated block, while other subcarriers are nulled out. To recover the transmitted and mapped data, an FFT is performed first, and then the square-law envelope detector is applied to estimate the active frequency index to recover the mapped bits, followed by a conventional demodulation to demodulate the transmitted bits. Furthermore, energy efficiency and complexity analyses have been carried out and it has been shown that PAPR is decreased in such a structure, which demonstrates the appropriateness of our system for WSN applications, where power and complexity must be kept at low profiles. Moreover, closed-form expressions of the BER performance over Rayleigh fading channels are derived. The proposed modulation scheme meets the needs of 5G wireless systems to a great extent, reduces PAPR, minimizes the consumed power, operates using a low latency and power profile and shows a promising overall performance. Future works will focus on advanced multiple access techniques incorporating frequency index modulation schemes.

REFERENCES

- [1] P. Pirinen, "A brief overview of 5G research activities," in *Proc. 1st IEEE Int. Conf. 5G Ubiquitous Connectivity (5GU)*, Nov. 2014, pp. 17–22.
- [2] P. Rawat, K. D. Singh, H. Chaouchi, and J. M. Bonnin, "Wireless sensor networks: A survey on recent developments and potential synergies," *J. Supercomput.*, vol. 68, no. 1, pp. 1–48, 2014.
- [3] J. Abouei, K. N. Plataniotis, and S. Pasupathy, "Green modulation in dense wireless sensor networks," in *Proc. IEEE Int. Conf. Acoust., Speech Signal Process*, Mar. 2010, pp. 3382–3385.
- [4] R. Mesleh, H. Haas, C. W. Ahn, and S. Yun, "Spatial modulation—A new low complexity spectral efficiency enhancing technique," in *Proc. 1st IEEE Int. Conf. Commun. Netw. (ChinaCom)*, Oct. 2006, pp. 1–5.
- [5] R. Y. Mesleh, H. Haas, S. Sinanovic, C. W. Ahn, and S. Yun, "Spatial modulation," *IEEE Trans. Veh. Technol.*, vol. 57, no. 4, pp. 2228–2241, Jul. 2008.
- [6] J. Jeganathan, A. Ghayeb, and L. Szczecinski, "Spatial modulation: Optimal detection and performance analysis," *IEEE Commun. Lett.*, vol. 12, no. 8, pp. 545–547, Aug. 2008.
- [7] M. D. Renzo, H. Haas, A. Ghayeb, S. Sugiura, and L. Hanzo, "Spatial modulation for generalized MIMO: Challenges, opportunities, and implementation," *Proc. IEEE*, vol. 102, no. 1, pp. 56–103, Jan. 2014.
- [8] M. D. Renzo, H. Haas, and P. M. Grant, "Spatial modulation for multiple-antenna wireless systems: A survey," *IEEE Commun. Mag.*, vol. 49, no. 12, pp. 182–191, Dec. 2011.
- [9] H.-C. Chang, Y.-C. Liu, and Y. T. Su, "Detection of spatial-modulated signals in the presence of CSI error and time-spatial correlation," in *Proc. IEEE Globecom Workshops (GC Wkshps)*, Dec. 2013, pp. 82–86.
- [10] E. Soujeri and G. Kaddoum, "Performance comparison of spatial modulation detectors under channel impairments," in *Proc. IEEE Int. Conf. Ubiquitous Wireless Broadband (ICUBW)*, Oct. 2015, pp. 1–5.
- [11] E. Soujeri and G. Kaddoum, "The impact of antenna switching time on spatial modulation," *IEEE Wireless Commun. Lett.*, vol. 5, no. 3, pp. 256–259, Jun. 2016.
- [12] G. Kaddoum, M. F. A. Ahmed, and Y. Nijssure, "Code index modulation: A high data rate and energy efficient communication system," *IEEE Commun. Lett.*, vol. 19, no. 2, pp. 175–178, Feb. 2015.
- [13] R. Abu-Alhiga and H. Haas, "Subcarrier-index modulation OFDM," in *Proc. 20th IEEE Int. Symp. Pers., Indoor Mobile Radio Commun.*, Sep. 2009, pp. 177–181.
- [14] D. Tsonev, S. Sinanovic, and H. Haas, "Enhanced subcarrier index modulation (SIM) OFDM," in *Proc. IEEE GLOBECOM Workshops (GC Wkshps)*, Dec. 2011, pp. 728–732.
- [15] E. Başar, Ü. Aygözü, E. Panayirci, and H. V. Poor, "Orthogonal frequency division multiplexing with index modulation," *IEEE Trans. Signal Process.*, vol. 61, no. 22, pp. 5536–5549, Nov. 2013.
- [16] E. Başar, "Multiple-input multiple-output OFDM with index modulation," *IEEE Signal Process. Lett.*, vol. 22, no. 12, pp. 2259–2263, Dec. 2015.
- [17] P. Barnaghi, W. Wang, C. Henson, and K. Taylor, "Semantics for the Internet of Things: Early progress and back to the future," *Int. J. Semantic Web Inf. Syst.*, vol. 8, no. 1, pp. 1–21, 2012.
- [18] J. G. Proakis, *Digital Communications*. New York, NY, USA: McGraw-Hill, 2001.
- [19] P. Elavarasan and G. Nagarajan, "A summarization on PAPR techniques for OFDM systems," *J. Inst. Eng. Ser. B*, vol. 96, no. 4, pp. 381–389, 2015. [Online]. Available: <http://dx.doi.org/10.1007/s40031-014-0156-2>
- [20] S. H. Han and J. H. Lee, "An overview of peak-to-average power ratio reduction techniques for multicarrier transmission," *IEEE Wireless Commun.*, vol. 12, no. 2, pp. 56–65, Apr. 2005.
- [21] S. Litsyn, *Peak Power Control in Multicarrier Communications*. Cambridge, U.K.: Cambridge Univ. Press, 2007.
- [22] L. J. Cimini, Jr., B. Daneshmand, and N. R. Sollenberger, "Clustered OFDM with transmitter diversity and coding," in *Proc. IEEE Global Telecommun. Conf. (GLOBECOM)*, vol. 1, Nov. 1996, pp. 703–707.
- [23] L. J. Cimini, Jr., and N. R. Sollenberger, "OFDM with diversity and coding for advanced cellular Internet services," in *Proc. IEEE Global Telecommun. Conf.*, vol. 1, Nov. 1997, pp. 305–309.



EBRAHIM SOUJERI (M'03–SM'11) received the B.Sc., M.Sc., and Ph.D. degrees in electrical and electronics engineering from Eastern Mediterranean University (EMU), Famagusta, Northern Cyprus, in 1995, 1997, and 2003, respectively. He was with the Department of Electrical and Electronics Engineering, EMU, from 1996 to 2002, as a Research Assistant while pursuing the M.Sc. and Ph.D. degrees. In 2002, he was with the Department of Computer Engineering, Cyprus International University for one year. In 2003, he joined the Faculty of Engineering, European University of Lefke, Northern Cyprus. In 2007, he was a Visiting Assistant Professor with Sultan Qaboos University, Muscat, Oman. He was also with the Department of Computer Science and Software Engineering, Concordia University, Montreal, Canada, on part-time basis from 2012 to 2014. He has been pursuing a second Ph.D. degree with École de Technologie Supérieure, Montréal, QC, Canada, since 2014. His current research interests include wireless communication systems, spread spectrum, and index modulation techniques. He is a Reviewer of various IEEE journals and conferences.



GEORGES KADDOUM (M'11) received the bachelor's degree in electrical engineering from the Ecole Nationale Supérieure de Techniques Avancées, Brest, France, and the M.S. degree in telecommunications and signal processing (circuits, systems, and signal processing) from the Université de Bretagne Occidentale and Telecom Bretagne, Brest, in 2005, and the Ph.D. degree (Hons.) in signal processing and telecommunications from the National Institute of Applied Sciences, University of Toulouse, Toulouse, France, in 2009. Since 2013, he has been an Assistant Professor of electrical engineering with the Ecole de Technologie Supérieure (ETS), University of Quebec, Montreal, QC, Canada. In 2014, he received the ETS Research Chair in physical-layer security for wireless networks. Since 2010, he has been a Scientific Consultant in the field of space and wireless telecommunications for several U.S. and Canadian companies. In 2014, he received the ETS Research Chair in physical layer security for wireless networks. He has authored over 130 journal and conference papers and has two pending patents. His recent research activities cover mobile communication systems, modulations, secure transmissions, and space communications and navigation. He received the Best Paper Award at the 2014 IEEE International Conference on Wireless and Mobile Computing, Networking, and Communications, with three co-authors, and the 2015 and 2017 IEEE TRANSACTIONS ON COMMUNICATIONS Exemplary Reviewer Award. He is currently serving as an Editor for the IEEE COMMUNICATIONS LETTERS.



MINH AU received the B.S. and M.S. degrees in computer science and telecommunication from the University of Poitiers, Poitiers, France, in 2007 and 2010, respectively, and the Ph.D. degree from Ecole de technologie supérieure, Montreal, QC, Canada, in 2016. He is currently a Post-Doctoral Fellow with the Ecole de technologie supérieure, Montreal, QC, Canada. His current research interests include channel modeling in the electrical grid, partial discharge phenomenon, low-latency communication, information theory, and coding theory.



MARIJAN HERCEG (M'14) received the B.Sc. and Ph.D. degrees in the electrical engineering from the Faculty of Electrical Engineering, Computer Science and Information Technology Osijek, Croatia, in 2002 and 2010, respectively. He is currently an Associate Professor with the Department of Communications, Faculty of Electrical Engineering, Computer Science and Information Technology. His current research interests include advanced modulation techniques for impulse radio ultra-wideband systems and chaos-based communication systems, multiple access techniques, and sigma-delta A/D converters.

...